Arévalo-Sáenz *et al.*
Egyptian Journal of Neurosurgery (2022) 37:34
https://doi.org/10.1186/s41984-022-00172-y

Egyptian Journal of Neurosurgery

RESEARCH Open Access

High-grade glioma and solitary metastasis: differentiation by spectroscopy and advanced magnetic resonance techniques

Alejandra Arévalo-Sáenz[1*], Gregorio Rodríguez-Boto Amago[2] and Manuel Pedrosa Sánchez[3]

Abstract

Background: The differentiation by means of magnetic resonance between high-grade gliomas and intracranial solitary single metastasis is of the utmost importance since they condition both surgical and complementary treatment.

Results: Retrospective study that analyzes the parameters of advanced magnetic resonance imaging: spectroscopy, diffusion and perfusion, specifically focused on the differences in the coefficients of the metabolites Cho/Cr, Cho/NAA and NAA/Cr in peritumoral edema between high-grade gliomas and metastases. The data have been statistically analyzed using ROC (receiver operating characteristic) curves, and cutoff values were obtained.

A total of 79 patients with histologically analyzed tumors were analyzed: 49 high-grade gliomas (40 multiform glioblastomas and 9 anaplastic astrocytomas) and 30 metastases. A statistically significant mean difference was obtained in the three metabolite ratios. The area under the curve for the Cho/NAA ratio was 0.958 (CI: 0.903–1), for Cho/Cr 0.922 (CI: 0.859–0.985) and for NAA/Cr 0.163 (CI: 0.068–0.258; $p < 0.001$). The cutoff values were 1.115 for Cho/NAA (sensitivity 93.87%, specificity 93.33%, global precision 93.67%); 1.18 for the Cho/Cr ratio (sensitivity 89.79%, specificity 93.33% and precision 91.13%) and 1.155 for the NAA/Cr ratio (sensitivity 67.34%, specificity 93.33%, global precision 44.30%).

Conclusion: The results of the study support the premise that spectroscopy at the level of peritumoral edema is able to differentiate between high-grade gliomas and metastases by showing tumor infiltration in peritumoral edema.

Keywords: Metastasis, High-grade gliomas, Magnetic resonance, Spectroscopy, Glioblastoma multiforme

Background

Brain metastases are the most common intracranial tumors, affecting 20–40% of cancer patients. Its main form of presentation is as a single intracranial mass. In this same way, high-grade primary brain tumors (glioblastoma multiforme and anaplastic astrocytomas) often present [1, 2]. Given the clear difference between the medical–surgical management and the survival of these two pathologies, its diagnosis prior to surgery is of vital importance. Magnetic resonance imaging (MRI) is the fundamental diagnostic tool available to the neurosurgeon for this purpose.

For many years, conventional techniques have had limitations in this regard, given the similarities in the presentation of these two pathologies. With the arrival of advanced techniques (spectroscopy, perfusion and diffusion), anatomical information is combined with physiological and metabolic information, and in this way, the differentiation between the two begins to glimpse a way out [3].

The purpose of this article is to analyze different advanced MRI parameters and characterize the efficacy of each one of them in the differentiation of these two pathologies.

*Correspondence: praimale@hotmail.com

[1] Division of Neurosurgery, Neurosurgery Department, Hospital Clinico San Carlos, Hospital QuironSalud, C / Profesor Martín Lagos S/N, 28040 Madrid, Spain
Full list of author information is available at the end of the article

Methods

A retrospective analysis was performed about brain tumor cases operated at the Neurosurgery Service of the Hospital Universitario de la Princesa from 2016 to 2018.

The selection criteria were the presence of a single intracranial tumor lesion and the performance of advanced pre-surgical imaging techniques. The presence of spectroscopy was considered mandatory, the presence of diffusion or perfusion being optional. Patients with a previous history of surgery, radiotherapy or chemotherapy or with more than one lesion were excluded.

A total selection of 79 patients was obtained. Advance MRI techniques were performed prior patients consent.

MRI imaging technique

The image was taken with a Siemens 1.5 T system (Magnetom Sonata; Siemens, Erlangen, Germany). The MRI imaging protocol included T2- and T1-weighted pre-contrast transverse echo-spin images. In each study, T2-weighted images were obtained using a rotational echo sequence with a TR/TE of 4000/100 and a slice thickness of 3 mm. T1-weighted pre-contrast images were acquired with a slice thickness of 3 mm and a TR/TE of 800/9.

Spectroscopy

Spectroscopic data were obtained after administration of gadopentetate dimeglumine. Three-dimensional selective excitation was used to excite a rectangular section, and the size of the section depended on the location and size of the lesion. The section was positioned in the peritumoral region and the normal contralateral brain parenchyma as a control, avoiding contamination of the scalp fat. The peritumoral region was defined within 1 cm outside the external tumor margin [4].

Spectral maps were obtained with an 8×8 matrix, having a voxel size of 1×1x1.5 cm, or 1×1x2 cm, depending on the thickness of the section. The term "spectroscopic MR imaging" is used synonymously with multivoxel spectroscopy, MR spectroscopic imaging or chemical shift imaging spectroscopy. All spectroscopic MR studies were multivoxel and/or chemical shift acquisitions and/or MR spectroscopy imaging.

Data processing

Spectroscopic data were processed using an offline workstation with standard software (Siemens). The spectral data were automatically corrected, except for the cases that seemed distorted in which the manual method was used.

The Gaussian filters were automatically adjusted to the peaks of choline (Cho), creatinine (Cr) and N-acetylaspartate (NAA), and the following coefficients were calculated: Cho/NAA; Cr/NAA; and Cho/Cr. The lipid and lactate (LL) peaks were also obtained in addition to the possible myoinositol (MI) peaks.

The metabolic relationships in the multiple voxels were calculated; however, only the maximum values in three locations were included, depending on the metabolite to be analyzed (intratumoral, the peritumoral region and in the normal contralateral brain parenchyma), and the spectra with these maximum values were identified from spectral maps.

Metabolite values were automatically calculated from the area under each metabolite peak using the standard commercial software program provided by the manufacturer. The integral peak values were normalized to the internal Cr peak.

Statistic analysis

The metabolic ratios obtained from spectroscopic MRI data between high-grade gliomas and metastases were compared using Student's t test. A P value less than 0.05 indicated a statistically significant difference.

The comparison between the different proportions in the expression of different metabolites such as LL, general decrease in metabolites or increase in myoinositol was calculated using Fisher's exact test. This test has a significant level of 5%. An analysis of the results was also carried out using the ROC curve (reception operating curve). Analyses based on logistic regression models were used to find the optimal cutoff value (sensitivity/specificity ratio) for metabolite ratios in order to achieve the most accurate diagnostic prediction possible. The area under the curve or AUC was taken as a criterion. AUC values of 51–70%, 71–90%, and > 90% indicate low, moderate and high diagnostic accuracy, respectively. Sensitivity (S), specificity (E), positive predictive value (PPV), negative predictive value (NPV) and precision for optimal thresholds were subsequently detailed. Precision was defined as the number of truly identified patients divided by the total number of cases. The Statistical Package for the Social Sciences software (Version 15.0; SPSS, Chicago, Illinois) was used for the analysis of statistical data.

Results

Descriptive analysis

The total selection consists of 79 patients (43 men, 36 women; ages between 30 and 85 years with a mean of 60.96 years). The predominant debut symptom was the seizure present in 28 patients, representing 35.4.9% of the total, and the second most frequent was the onset with paresthesia or hemiparesis present in 15 patients (19%). You can see the distribution in Table 1

Table 1 Description of the initial symptoms of the study patients in which it can be seen that the epileptic seizure is the most frequent symptom

Patients symptoms	Frequency	Percentage (%)
Epileptic seizures	28	35.4
Headache/vomiting/nausea	10	12.7
Paresthesia/hemiparesis	15	19
Language impairment	7	8.9
Vision impairment	1	13
Gait disturbance	6	7.6
Behavior alteration	5	6.3
Disorientation	2	2.5
Casual	1	1.3
General impairment	3	3.8
Others	1	1.3

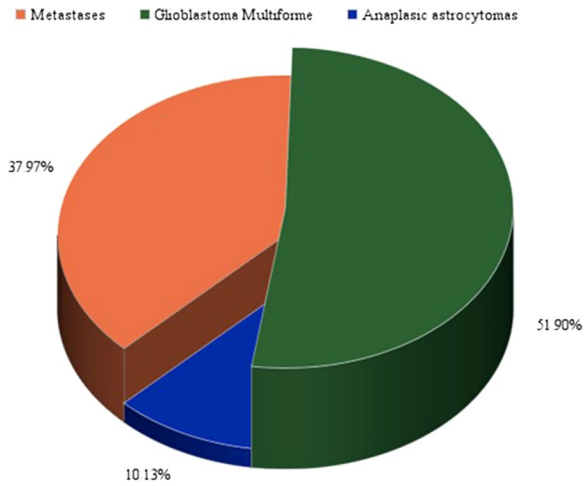

Fig. 1 Description of the percentage of the different tumor types in the study

The lesions were distributed in different locations, predominantly the frontal lesion in 30 patients (38%) and the pure temporal lesion in 17 patients (24.1%).

The lesions were distributed in practically the same proportion between the right and left hemispheres (48.1% and 46.8%). Four patients presented central location with bilateral extension (5.1%).

Spectroscopy studies were performed in 79 patients, perfusion studies were performed in 79 patients, diffusion studies were performed in 76 patients, and anisotropy studies were performed in 72.

In a total of 69 patients, a complete study was performed using spectroscopy, diffusion, perfusion and anisotropy: 39 patients with primary tumors and 30 patients with metastases. The radiologist was responsible for the choice of advanced MRI techniques.

The pathological examination revealed that 49 patients histologically presented a high-grade tumor (glioblastoma multiforme) and anaplastic forms (AA) according to the classification of the World Health Organization. Of the 49 patients with high-grade tumors, 41 corresponded to glioblastoma multiforme and 8 to anaplastic astrocytoma. Of the 30 patients with metastases, 2 were derived from gastrointestinal tumors, 6 from breast cancer, 1 from the ovary, 2 from melanoma, 2 from the pancreas and 16 from the lung (adenocarcinoma, neuroendocrine and small cells). Seventy-two open surgeries (88.3%) and 7 biopsies (11.7%) were performed. Results are shown in Fig. 1.

Statistic analysis

A comparison was made between coefficients of metabolites found in peritumoral edema.

The mean of the Cho/Cr coefficient in high-rank and metastatic gliomas was: 1.5931 ± 0.4248 and 0.9201 ± 0.1964, whose difference was statistically significant ($p < 0.001$).

The mean of the Cho/NAA coefficient between high-ranking gliomas and metastases was: 1.4845 ± 0.40881 and 0.7697 ± 0.2302, whose differences were statistically significant ($p < 0{,}001$).

The mean of the NAA/Cr coefficient among high-ranking and metastatic gliomas was: 1.1857 ± 0.089 and 1.289 ± 0.0839, whose differences were not significant (p: 0.05).

The data are synthesized in Table 2.

By making the disaggregated comparisons between GBM/metastasis and AA/metastasis, significant indices were also obtained at the level of peritumoral edema except in the NAA/Cr coefficient. The results can be viewed in Table 3.

The comparison made between AA and GBM did not yield any significant data.

Lipids and lactates: Intratumor expression of lipids (at 0–9 and 1–3 ppm) and lactate (1.35 ppm) was detected both at the level of high-grade gliomas and metastases. The proportion within the GBM/AA group was 44 cases with a positive peak (GBM: 40, AA: 4) and 5 with a negative peak. In the metastasis group, the relationship was 27 positives versus 3 negatives. No statistically significant differences were found when the chi-square test was performed, so this metabolite does not serve to differentiate both pathologies.

Other variables

Regarding the generalized decrease in metabolites, it was found that 14 of 48 high-grade gliomas presented it. Regarding metastases, they were 6 out of 30. These data

Table 2 Results of the MRS coefficients in peritumoral edema in high-grade gliomas and metastases

Tumor group	Cho/Cr mean (± SD)	Cho/NAA mean (± SD)	NAA/Cr mean (± SD)
High-grade gliomas (*n*:49)	1.59 ± 0.42	1.48 ± 0.41	1.19 ± 0.09
GBM (*n*:40)	1.57 ± 0.43	1.53 ± 0.42	1.18 ± 0.70
AA (*n*:8)	1.68 ± 0.41	1.28 ± 0,30	1.22 ± 0.15
Metastases	0.92 ± 0.19	0.77 ± 0.23	1.29 ± 0.08

SD standard deviation

Table 3 Comparison of MRS coefficients in peritumoral edema for high-grade gliomas, GBM, AA and metastases

Comparison	Cho/Cr	Cho/NAA	NAA/Cr
High-grade gliomas versus metastases	*P* < 0.0001	*P* < 0.0001	*P*: 0.05
GBM versus metastases	*P* < 0.0001	*P* < 0.0001	*P*: 0.209
AA versus metastases	*P*: 0.005	*P*: 0.004	*P*: 1.49

are not significant and do not show a characteristic profile of either of these two pathologies. The analysis was also not significant when performed by subgroups.

There was a slight statistically positive difference (*p*: 0.049) between the expression of a myoinositol peak between the AA group and the GBM group.

ROC curves

By making a comparison between the three metabolite coefficients, we can deduce that Cho/NAA has greater discriminative power than the other tests in the identification of high-grade gliomas versus metastases: area under the curve (confidence interval) 0.958 (CI: 0,903–1 vs. Cho/Cr 0.922 (CI: 0.859–0.985) and NAA/Cr 0.163 (CI: 0.068–0.258; $p < 0.001$ (Fig. 2).

The NAA/Cr coefficient presents an area under the curve of 0.837 (0.742–0.932) in the identification of metastases against high-grade gliomas (Fig. 3).

Optimal cutoff values

ROC analysis for the differentiation between metastasis and high-grade gliomas yielded an optimal cutoff value of 1.115 for the peritumoral Cho/NAA ratio variable. This implies a proportion of correctly identified high-grade gliomas (sensitivity) of 93.87%, a proportion of correctly identified metastases (specificity) of 93.33%, the proportion of true high-grade gliomas identified as such (PPV) was 95.83% and the proportion of true metastases identified as such (NPV) was 95.83%.The overall test precision was 93.67%

The cutoff value for other variables was > or equal to 1.18 for the Cho/Cr coefficient (sensitivity of 89.79%, specificity of 93.33%, positive predictive value of 95.65%

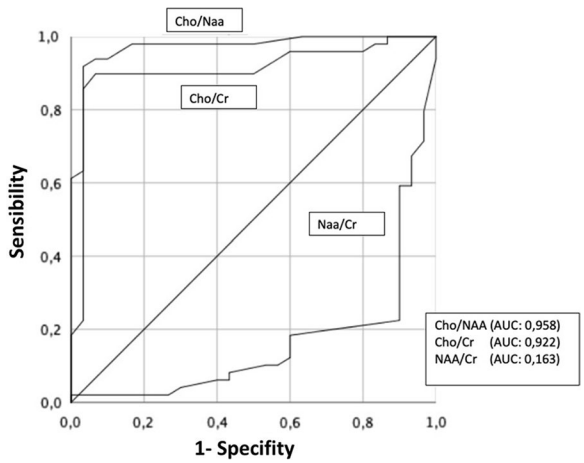

Fig. 2 Graph showing a ROC (receiving operating characteristic) curve of the peritumoral variables Cho/NAA, Cho/Cr and NAA/Cr for the differentiation of high-grade gliomas and metastases. This graph shows the discriminative capacity of each variable, also providing the areas under the curve (AUC)

and negative predictive value of 84.84% and a precision of 91.13%) and 1.155 for the NAA/Cr coefficient (sensitivity of 67.34%, specificity of 93.33%, PPV of 54.09%, NPV of 11.11% and global precision of 44.30%). For the Cho/Cr and Cho/NAA variables, a high value of the coefficient corresponds to high-grade gliomas and a low grade to metastasis. On the contrary, a high value of the NAA/Cr coefficient corresponds to metastasis (Fig. 4).

The details of the ROC curves are shown in Table 4.

Perfusion

A qualitative analysis was performed. An increase in global arterial flow was found in 45/49 high-grade gliomas and in 17/30 metastases. The difference was significant *p*: 0.002.

The most frequent found pattern was peripheric increase and central decrease in arterial flow. This pattern was expressed in 17/49 high-grade gliomas and in only 1 metastasis. This difference was statistically significant.

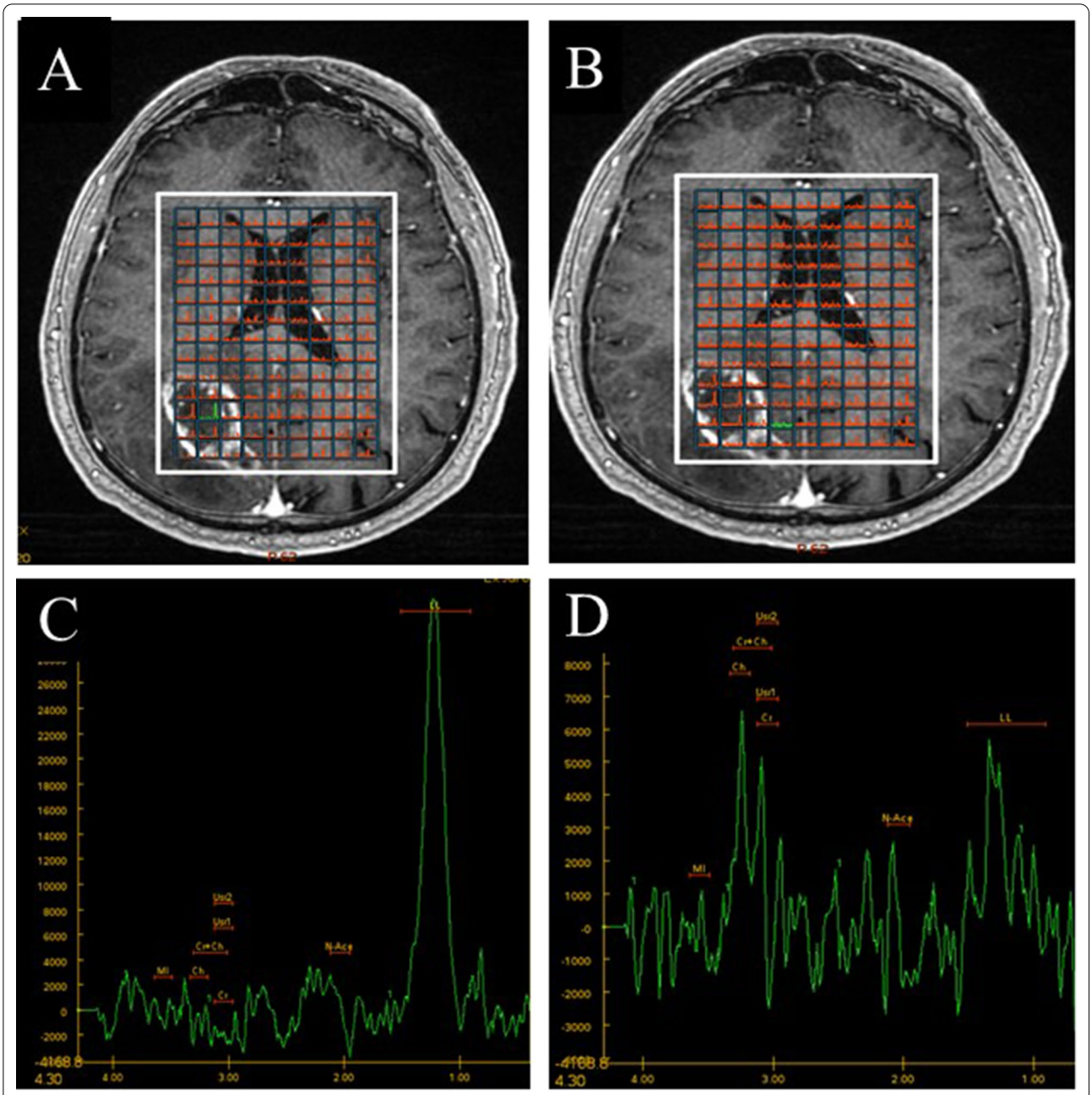

Fig. 3 A 68-year-old male patient with a brain tumor in the right parietal region confirmed histologically as a grade IV astrocytic tumor (astrocytoma). **A** and **B** axial MR image in T1 sequence with contrast. A heterogeneous lesion with irregular ring-shaped enhancement and central necrosis can be seen. Perilesional edema is noted in the form of hypodensity in T1 sequence (vasogenic edema and tumor infiltration); **C** spectroscopy of the tumor area with elevated lipids and lactates in addition to a generalized decrease in the rest of the metabolites; typical of areas with necrosis and ischemia; **D**: spectroscopy of the peritumoral area with a characteristic pattern of increased Cho and Cr together with decreased NAA

Anisotropy

A qualitative analysis was performed. The anisotropy study was present in 72 of 79 patients. Fifty-four patients had a loss of local fractional anisotropy or brain microstructure. When comparing groups, a statistically significant difference was found with a trend of greater local aggressivity for high-grade glioma group.

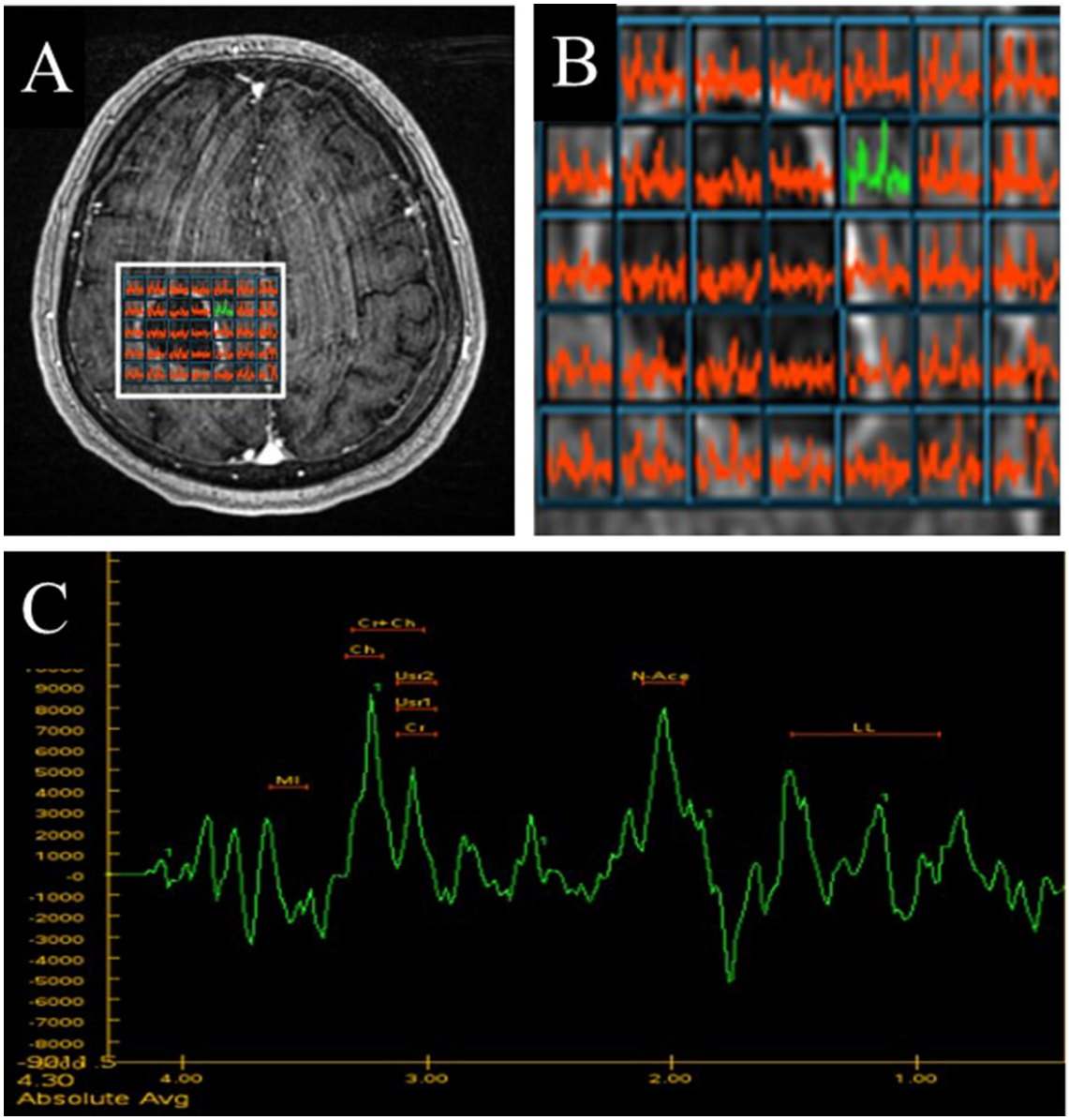

Fig. 4 A 57-year-old male patient with a histologically confirmed right prerolandic frontal lesion as metastasis from lung cancer. **A** Axial T1-weighted MR image with contrast. An irregular linear peripheral enhancement lesion with thickenings is visualized; **B** spectroscopic map in which the lack of choline elevation in the peritumoral voxels can be confirmed; **C** spectroscopic analysis showing a Cho peak and a not so pronounced NAA drop

Table 4 Measures of sensitivity, specificity, positive predictive value, negative predictive value, cutoff values (CV) and precision using MRS coefficients in peritumoral edema for discrimination of high-grade gliomas and metastases using ROC curve analysis

Parameter	CV	Sensitivity%	Specificity%	PPV%	NPV%	AUC	Precision
Cho/Cr	1.18	89.79%	93.33%	95.65%	84,.4%	92.2%	91.13%
Cho/NAA	1.115	93.87%	93.33%	95.83%	95.83%	95.8%	93.67%
NAA/Cr	1.155	67.34%	93.33%	54.09%	11.11%	16.3%	44.30%

Discussion

Solitary metastatic lesions are virtually indistinguishable from high-grade gliomas on basic MRI sequences. Carrying out this differential diagnosis preoperatively is important both for surgical planning and for follow-up and complementary treatment modalities. Some patients with poor general condition or with many comorbidities could benefit from the absence of a biopsy, since the performance of this technique often involves the repetition of the procedure. MRS is a technique that provides semiquantitative in vivo information on the metabolic composition of different CNS lesions [5]. The measurement of the different metabolites allows not only the differentiation of intracranial lesions, but also their tumor grading as well as assessing tumor viability and the state of the cell membrane and its turnover [6]. The spectroscopic pattern present in tumor lesions is characterized by a decrease in NAA with an increase in Cho levels, and lipids and lactates can be found in the tumor center due to necrosis or areas of ischemia produced by its rapid growth [5]

In our study, both the Cho/Cr and Cho/NAA coefficients obtained in peritumoral edema were statistically different between both pathologies. These differences in the peritumoral area associated with each tumor type can be explained by its different pathophysiologies [7, 8]: abnormalities in the tumor endothelium, secretion of the tumor vascular growth factor, tumor angiogenesis, etc. In high-grade gliomas, the areas of peritumoral tumors show, in addition to morphologically altered capillaries and interstitial water, infiltrating tumor cells along preexisting dilated vascular channels and those formed de novo. In metastatic edema, the edema is purely vasogenic, consisting of fluid without tumor cells, a fact that does not occur in high-grade glioma edema [9, 10]. It should be noted that the different behavior between high-grade and metastases also conditions an increase in Cho at the peritumoral level at the tumor level (prima necrosis). Cho is a faithful marker of the increase in membrane synthesis and therefore of cell multiplication [11]. The Cho/Cr index and the Cho/NAA are markers of degree of malignancy [12]. We have based our study on these differences in peritumoral behavior.

Our findings are consistent with previous studies, observing a higher Cho/Cr ratio in peritumoral edema when comparing high-grade gliomas versus metastasis [13, 14]. Among the most important studies, the one carried out by Server et al. [15] in 2010 with a significant difference was obtained in Cho/NAA, Cho/Cr and NAA/Cr coefficients in peritumoral edema between high-grade gliomas and metastases. In the same way, in the article by Weber et al. [16] an elevation in Cho/NAA ratios in the hyperintense perifocal T2 region was reported in high-grade gliomas, in contrast to the lack of elevation in metastases.

Regarding the use of other indices, two renowned authors such as Chiang et al. and Law et al. [13, 14] did not find a statistical difference in the peritumoral analysis of the NAA/Cr coefficient between high-grade gliomas and metastases, a validated result, by our study. This absence of difference between the two pathologies may be due to the absence of neuronal replacement or destruction in peritumoral areas. In high-grade gliomas, tumor cells infiltrate along the vascular channels but do not destroy the preexisting cytoarchitecture [17]. On the other hand, vasogenic edema associated with metastasis is a passive process that does not necessarily destroy the underlying structure or neural tissue [18]

We must not forget that N-acetyl aspartate or NAA is a neuronal marker and creatinine or Cr is a molecule that plays an important role in the maintenance of energy-dependent systems in brain cells. A low NAA/Cr coefficient is a reliable indicator of malignancy, and this decrease is also quantifiable with significant differences between gliomas of different grades [19].

Other authors have performed the spectroscopic analysis intratumorally rather than peritumorally. In our study, we have decided to do the analysis with the placement of the diagnostic voxel within the peritumoral area because it has been shown that it is less critical and that the degree of mixtures of the different types of tissue does not have significant implications for the calculated measurements, not being the case tumorally. Nelson et al. [20] in their study that it is difficult to obtain valid intratumoral spectra without partial tumor volume and necrosis due to the effects of tumor heterogeneity.

Regarding the presence of the lipid peak (tumor necrosis reflex), there are several studies [21, 22] that reflect its existence both at the level of high-grade gliomas and metastasis due to the generation of tumor necrosis. This is in line with our results as we did not find significant differences. In another more recent study, they have found that the signal of a lipid macromolecule allows significant discrimination between both pathologies [23].

In our study, sensitivities of 93.87% and 89.79% were found for the Cho/NAA and Cho/Cr ratios together with area under the curve of 0.958 and 0.922, respectively. This allows us to deduce that given the sensitivity and the area under the curve, the Cho/NAA parameter is more discriminative, although both parameters have very good discrimination. In the literature, different sensitivity values are shown according to the cutoff number value. Against our cutoff point of > 1.114 for Cho/NAA (S: 93.87%), Al-Okaili et al. [24] in 2007 obtained a cutoff point of > 1 (S: 83.33%); Cai et al. in 2009 [25] obtained a cutoff point of > 1.085 (S: 93.75%) and finally in 2010 it

was Server et al. [15] and Wong et al. [26] who obtained cutoff points of > 1.11 (S: 91.11%) and > 1 (S: 88.88%), respectively. Given these data, we can say that our analysis goes in the same direction as the literature.

Regarding the analysis of the Cho/Cr coefficient in the literature, compared to our > 1.17 with S: 89.79%, we found Cai et al. in 2009 [25] with a cutoff point of > 1.032 (S: 81.21%) and Server et al. and Chawla S. et al. [27] in 2010 with cutoff points of > 1.21 (S: 88.88%) and > 0.4 (S: not reported), respectively. We clearly realize that the sensitivity of this coefficient is less than that of Cho/NAA, which in our opinion is the one of the choices in the first instance.

Finally, making a review of the NAA/Cr coefficient values in the literature, we find that compared to our 1,155 (S: 67.34%) Server et al. [15] provide a coefficient of 1.17 with a sensitivity of 68.88%. As we have previously explained, this coefficient is more effective in detecting metastasis vs gliomas than applying it the other way around. And this logical conclusion is also described in the literature. All this can be visualized in Table 5.

In addition to alterations at the level of metabolite coefficients, perfusion measured by rCBV at the peritumoral level also shows important differences between high-grade gliomas and metastases. In our study, we have carried out a qualitative study of perfusion; however, other authors such as Law et al. [14] have quantified the increase in perfusion up to 1.39 higher than normal white matter in contrast to perfusion in metastasis which was 0.39 (less than normal white matter).

At present, there are already published studies with diagnostic strategies based on advanced resonance techniques [27]. In this strategy, they combine spectroscopy, diffusion and enhancement of the lesion to make a first approximation. The final differentiation between high-grade gliomas and metastases is based on a Cho/NAA coefficient greater or less than 1. The global precision of this study estimates that with combined imaging techniques the diagnosis can be reached preoperatively in 85–90% of intraaxial lesions.

Our study has a limitation, which is found in all the studies with spectroscopic analysis, which is the effects of tumor heterogeneity whereby the metabolite signal can be influenced in some cases by the partial effect of volume.

Conclusion

In conclusion, our study shows that through advanced spectroscopy techniques the differentiation between high-grade gliomas (GBM and AA) and metastases, especially when measurements of the Cho/Cr and Cho/NAA ratios are included in peritumoral edema, is possible with high precision. In this case, a coefficient greater than 1.59 in the Cho/Cr ratio and 1.48 in Cho/NAA orients the diagnosis of high glioma vs metastasis with very high sensitivity and specificity.

Abbreviations

AA: Anaplastic astrocytomas; AUC: Area under the curve; Cho: Choline; CI: Confidence interval; Cr: Creatinine; CV: Cutoff value; E: Specificity; GBM: Glioblastoma multiforme; LL: Lipids and lactate; MI: Myoinositol; MRI: Magnetic resonance imaging; MRS: Magnetic resonance spectroscopy; NAA: N-acetylaspartate; NPV: Negative predictive value; PPV: Positive predictive value; rCBV: Relative cerebral blood volume; ROC: Receiver operating characteristic; ROI: Region of interest; S: Sensitivity; TE: Echo time; TR: Repetition time.

Acknowledgements

Not applicable.

Author contributions

AA analyzed and interpreted the patient data and prepared the manuscript. GD and MP performed the review of the images and cases and reviewed the manuscript data and references. Both operated many of the cases analyzed. All authors read and approved the final manuscript.

Funding

Not applicable. No funding was used in this study.

Availability of data and materials

The databases used during the current study are available from the corresponding author on reasonable request.

Table 5 Comparison of the different cutoff points in the literature providing means of sensitivity, specificity, positive predictive value, negative predictive value and precision

	Cho/NAA		Cho/Cr		NAA/Cr	
Study	**CV**	**Sensibility**	**CV**	**Sensibility**	**CV**	**Sensibility**
Our study	> 1.114	93.87%	> 1.17	89.79%	> 1.154	67.34%
Al-Okaili et al. [18] 2007	> 1	83.33%	–	–	–	–
Cai et al. [19] 2009	> 1.085	93.75%	> 1.032	81.21%	–	–
Server et al. [10] 2010	> 1.11	91.11%	> 1.21	88.88%	> 1.17	68.88%
Wong et al. [20] 2010	> 1	88.88%	–	–	–	–
Chawla. S et al. [21] 2010	–	–	> 0.4	NA	–	–

NA available

Declarations

Ethics approval and consent to participate
Not applicable.

Consent for publication
Not applicable.

Competing interests
The authors declare that they have no competing interests.

Author details
[1]Division of Neurosurgery, Neurosurgery Department, Hospital Clinico San Carlos, Hospital QuironSalud, C / Profesor Martín Lagos S/N, 28040 Madrid, Spain. [2]Department of Neurosurgery, Puerta de Hierro University Hospital, C / Joaquín Rodrigo, 1, 28222 Majadahonda, Madrid, Spain. [3]Department of Neurosurgery, Hospital Universitario de La Princesa, Hospital Sanitas La Moraleja, Hospital Sanitas La Zarzuela, C / Diego de León 62, 28006 Madrid, Spain.

Received: 12 January 2021 Accepted: 14 April 2021
Published online: 26 September 2022

References

1. Nguyen TD, DeAngelis LM. Brain metastases. Neurol Clin. 2007;25:1173–92. https://doi.org/10.1016/s0733-8619(02)00035-x.
2. Landis SH, Murray T, Bolden S, Wingo PA. Cancer statistics 1999. CA Cancer J Clin. 1999;49:8–31. https://doi.org/10.3322/canjclin.49.1.8.
3. Bulakbsi N, Kocaogly M, Ors F, Tayfun C, Ucoz T. Combination of single-voxel proton MR spectroscopy and apparent diffusion coefficient calculation in the evaluation of common brain tumors. AJNR Am J Neuroradiol. 2003;24(2):225–33 (**PMID: 12591638**).
4. Knopp EA, Cha S, Johnson G, et al. Glial neoplasms: dynamic contrast enhanced T2-weighted MR imaging. Radiology. 1999;211:791–8. https://doi.org/10.1148/radiology.211.3.r99jn46791.
5. Brandao LA, Domingues RC. Intracranial neoplasms. En: MR spectroscopy of the brain. Capitulo 10, LWW, Philadelphia, USA. 2004; p. 130–67.
6. Hollingworth W, Medina LS, Lenkinski RE, Shibata DK, Bernal B, Zurakowski D, et al. A systematic literature review of magnetic resonance spectroscopy for the characterization of brain tumors. AJNR. 2006;27:1404–11.
7. Zhang M, Olsson Y. Hematogenous metastases of the human brain-characteristics of peritumoral brain changes: a review. J Neurooncol. 1997;35:81–9. https://doi.org/10.1023/a:1005799805335.
8. Shibata S, Fukushima M, Inone M, Tsutsumi K, Mori K. Ultrastructure of capillary permeability in human brain tumors. Part 1: gliomas associated with cerebral edema (low density areas). No Shinkei Geka. 1985;13(3):275–81.
9. Bertossi M, Virgintino D, Maiorano E, Occhiogrosso M, Roncali L. Ultrastructural and morphometric investigation of human brain capillaries in normal and peritumoral tissues. Ultrastruct Pathol. 1997;2:41–9. https://doi.org/10.3109/01913129709023246.
10. Cha S, Lupo JM, Chen MH, Lamborn KR, McDermott MW, Berger MS, et al. Differentiation of glioblastoma multiforme and single brain metastases by peak height and percentage of signal intensity recovery derived from dynamic susceptibility-weighted contrast-enhanced perfusion MR imaging. Am J Neuroradiol. 2007;28:1078–84. https://doi.org/10.3174/ajnr.A0484.
11. Poptani H, Gupta RK. Characterization of intracranial mass lesions. Within vivo proton MR spectroscopy. AJNR Am J Neuroradial. 1995;16:1593–603.
12. Moller-Hartmann W, Herminghaus S, Krings T. Clinical application of proton magnetic resonance spectroscopy in the diagnosis of intracranial mass lesion. Neuroradiology. 2002;44:371–81. https://doi.org/10.1007/s00234-001-0760-0.
13. Chiang IC, Kuo YT. Distinction between high-grade gliomas and solitary metastases using peritumoral 3T magnetic resonance spectroscopy, diffusion, and perfusion imaging. Neuroradiology. 2004;46:619–27. https://doi.org/10.1007/s00234-004-1246-7.
14. Law M, Cha S, Knopp EA, Johnson G, Arnett J, Litt AW. High-grade gliomas and solitary metastases: differentiation by using perfusion and proton spectroscopic MR imaging. Radiology. 2002;222:715–21. https://doi.org/10.1148/radiol.2223010558.
15. Server A, Josefsen R, Kulle B, Maehlen J, Schellhorn TR, Gadmar O, et al. Proton magnetic resonance spectroscopy in the distinction of high-grade cerebral gliomas from single metastatic brain tumors. Acta Radiol. 2010;51:316–25. https://doi.org/10.3109/02841850903482901.
16. Weber MA, Zoubaa S, Schlieter M, Jüttler E, Huttner HB, Geletneky K, et al. Diagnostic performance of spectroscopic and perfusion MRI for distinction of brain tumors. Neurology. 2006;66:1899–906. https://doi.org/10.1212/01.wnl.0000219767.49705.9c.
17. Knopp EA, Cha S, Johnson G, Mazumdar A, Golfinos JG, Zagzag D, et al. Glial neoplasms: dynamic contrast-emhanced T2 weighted MR imaging. Radiology. 1999;211:791–8. https://doi.org/10.1148/radiology.211.3.r99jn46791.
18. Zhang M, Olsson Y. Hematogenous metastases of the human brain: characteristics of peritumoral brain changes- a review. J Neurooncol. 1997;35:81–9.
19. Möller-Hartmann W, Herminghaus S, Krings T, Marquardt G, Lanfermann H, Pilatus U, et al. Clinical application of proton magnetic resonance spectroscopy in the diagnosid of intracranial mass lessions. Neuroradiology. 2022;44:371–438. https://doi.org/10.1007/s00234-001-0760-0.
20. Nelson SJ. Multivoxel magnetic resonance spectroscopy of brain tumors. Mol Cancer Ther. 2003;2:497–507.
21. Shimaru H, Morikawa M, Iwanaga S, Kaminogo M, Ochi M, Hayashi K. Differentiation between high-grade glioma and metastatic brain tumor using single-voxel proton MR spectroscopy. Eur Radiol. 2001;11:1784–91. https://doi.org/10.1007/s003300000814.
22. Sijens PE, Knopp MV, Brunetti A, Wicklow K, Alfano B, Bachert P, et al. 1 HMR spectroscopy in patients with metastatic brain tumors: a multicenter study. Magn Reson Med. 1995;33:818–26. https://doi.org/10.1002/mrm.1910330612.
23. Opstad KS, Murphy MM, Wilkins PR, Bell BA, Griffiths JR, Howe FA. Differentiation of metastases from high-grade gliomas using short echo time 1 H spectroscopy. J Magn Reson Imaging. 2004;20:187–92. https://doi.org/10.1002/jmri.20093.
24. Al-Okaili RN, Krejza J, Woo JH, Wolf RL, O'Rourke DM, Judy KD, et al. Intraaxial brain masses: MR imaging-based diagnostic strategy—initial experience. Radiology. 2007;243:539–50. https://doi.org/10.1148/radiol.2432060493.
25. Cai J-Z, Cao D, Li Y, et al. The clinical value of PROBE-P 3D CSI of 1H-MRS in peritumoral region in differentiating highgrade primary gliomas and solitary metastasis. Chin J CT MRI. 2009;2:7–10.
26. Wong CS, Chu TYC, Ma JKF. Peri-tumoral magnetic resonance spectroscopy to differentiate solitary primary intra-axial high-grade glioma and brain metastasis: a pilot study. J Hong Kong Coll Radiol. 2010;13:195–8.
27. Chawla S, Zhang Y, Wang S, Chaudhary S, Chou C, O'Rourke DM, et al. Proton magnetic resonance spectroscopy in differentiating glioblastomas from primary cerebral lymphomas and brain metastases. J Comput Assist Tomogr. 2010;34:836–41. https://doi.org/10.1097/RCT.0b013e3181ec554e.

Publisher's Note